

Electroweak Vacuum Metastability and Low-scale Inflation

Yohei Ema,¹ Kyohei Mukaida,² and Kazunori Nakayama^{1,2}

¹*Department of Physics, Faculty of Science, The University of Tokyo*

²*Kavli IPMU (WPI), UTIAS, University of Tokyo, Kashiwa, 277-8583, Japan*

(Dated: July 3, 2022)

We study the stability of the electroweak vacuum in low-scale inflation models whose Hubble parameter is much smaller than the instability scale of the Higgs potential. In general, couplings between the inflaton and Higgs are present, and hence we study effects of these couplings during and after inflation. We derive constraints on the couplings between the inflaton and Higgs by requiring that they do not lead to catastrophic electroweak vacuum decay, in particular, via resonant production of the Higgs particles.

I. INTRODUCTION

The Higgs potential may have a deeper minimum than the electroweak (EW) vacuum once we assume that the Standard Model (SM) is valid up to a certain high-energy scale given the current observational results of the SM parameters. It does not mean any contradiction with the present universe since the allowed values of the SM parameters are likely to cause the metastable vacuum where the lifetime of the EW vacuum far exceeds the age of the universe [1–14].^{b1} Still, the existence of such a deeper minimum might cause problems in the early universe [19–25], especially during [26–38] and after inflation [39–44]. For instance, we can derive an upper bound on the inflation energy scale if there is no sizable coupling between the inflaton/the Ricci scalar and the Higgs during inflation. Otherwise, the Higgs acquires superhorizon fluctuations which are large enough to overcome the potential barrier during inflation. Thus, we assume that the EW vacuum is indeed metastable, and study its implications on dynamics during and after inflation in this paper.

Previous studies in this direction are performed mainly in the context of high-scale inflation. The reason is that the Hubble parameter during inflation H_{inf} must be at least comparable to the instability scale of the Higgs potential h_{inst} ($\sim 10^{10}$ GeV for the center values of the SM parameters) for inflation to have nontrivial effects on the EW vacuum, since otherwise superhorizon fluctuations during inflation are too small to overcome the potential barrier. However, the situation completely changes once we consider dynamics after inflation. After inflation, or during the inflaton oscillation epoch, the typical scale of the system is at least as large as the inflaton mass m_ϕ . Thus, as long as $m_\phi > h_{\text{inst}}$, even low-scale inflation that satisfies $h_{\text{inst}} \gg H_{\text{inf}}$ may threaten the metastable EW vacuum. This is possible because low-scale inflation models typically yield $m_\phi \gg H_{\text{inf}}$.

In this paper, we study dynamics of the Higgs during the inflaton oscillation epoch for low-scale inflation models with $m_\phi > h_{\text{inst}}$ and $m_\phi \gg H_{\text{inf}}$. In general, there are no reasons to suppress couplings between the inflaton and the Higgs. If these couplings are sizable, a resonant production of the Higgs particles occurs due to the inflaton oscillation, which is the so-called “preheating” phenomenon [45, 46]. The produced Higgs particles may force the EW vacuum to decay into the deeper minimum through the negative Higgs self-coupling. Thus we

may obtain tight upper bounds on the couplings by requiring that the EW vacuum survives the preheating epoch.

Previous studies on the preheating dynamics of the EW vacuum focused on high-scale inflation models [40–44] but there are some qualitative differences between high- and low-scale inflation models. For low-scale inflation models, one significant complexity arises due to the tachyonic instability of the inflaton fluctuation itself during the last stage of inflation and the subsequent inflaton oscillation epoch [47–50]. It can be efficient enough to break the homogeneity of the inflaton field before the Higgs field fluctuation develops. Our purpose in this paper is to derive the upper bounds on the Higgs-inflaton couplings in low-scale inflation models taking these effects into account.

This paper is organized as follows. In Sec. II, we explain our setup. Since low-scale inflation models typically correspond to small field inflation models, we concentrate on hilltop inflation models in this paper. In Sec. III, we briefly discuss the dynamics of the Higgs during inflation for low-scale inflation models. In Sec. IV, we study the preheating dynamics of the Higgs and inflaton itself, and qualitatively discuss the feature of the whole system. In Sec. V, we perform numerical simulations to derive bounds on the Higgs-inflaton couplings. Finally, Sec. VI is devoted to summary and discussions.

II. SETUP

In this section, we summarize our setup. We take the Lagrangian as

$$\mathcal{L} = \frac{M_{\text{Pl}}^2}{2} R - \frac{1}{2} (\partial \phi)^2 - \frac{1}{2} (\partial h)^2 - U(\phi, h), \quad (1)$$

where M_{Pl} is the reduced Planck scale, R is the Ricci scalar, ϕ is the inflaton, and h is the Higgs.^{b2} We assume that the inflaton is singlet under the SM gauge group, and hence trilinear as well as quartic portal couplings between the inflaton and the Higgs are allowed in general. Thus we take the following generic form for the potential:

$$U(\phi, h) = V(\phi) + \frac{\tilde{\sigma}_{\phi h}}{2} \phi h^2 + \frac{\lambda_{\phi h}}{2} \phi^2 h^2 + \frac{m_h^2}{2} h^2 + \frac{\lambda_h}{4} h^4, \quad (2)$$

where V is the inflaton potential, m_h^2 is the bare mass of Higgs, and $\tilde{\sigma}_{\phi h}$, $\lambda_{\phi h}$, and λ_h are coupling constants. Note that the

^{b1} For the gravitational correction, see *e.g.* Refs. [15–18] and references therein.

^{b2} We consider only one degree of freedom for simplicity. The results change only logarithmically even if we consider the full SU(2) doublet.

inflaton can have some gauge charges other than SM, such as $U(1)_{B-L}$. In that case, ϕ should be regarded as a radial component of the complex scalar, and $\tilde{\sigma}_{\phi h} = 0$. In this paper, however, we keep $\tilde{\sigma}_{\phi h} \neq 0$ to make our discussion generic. Also, although it is higher dimensional, the following term may be relevant:

$$\delta \mathcal{L}_{\text{kin}} = c_{\text{kin}} \frac{h^2}{M_{\text{Pl}}^2} (\partial \phi)^2. \quad (3)$$

It can be sizable, for it respects the shift symmetry, $\phi \rightarrow \phi + \text{const}$. We can also consider the non-minimal coupling between the Higgs and R . We first omit these terms for simplicity, and discuss their effects at the end of this paper.

Below we explain each term in detail.

A. Inflaton potential

As a prototype of an inflaton potential for low-scale inflation, we consider the hilltop model [51–54] (see Refs. [55–58] for supergravity embeddings):

$$V(\phi) = \Lambda^4 \left[1 - \left(\frac{\phi}{v_\phi} \right)^n \right]^2, \quad (4)$$

where $n > 2$ is an integer and $v_\phi > 0$ is the vacuum expectation value (VEV) of the inflaton at the minimum of its potential. The inflaton mass around the minimum is

$$m_\phi = \frac{\sqrt{2}n\Lambda^2}{v_\phi}. \quad (5)$$

Since we are interested in small field inflation models, we assume that $v_\phi \ll M_{\text{Pl}}$. Otherwise, the model would be rather similar to high-scale inflation models. Inflation takes place in the flat region of the potential: $|\phi| \ll v_\phi$. Here and in what follows, we consider the field space of the positive branch: $\phi > 0$.³ The Hubble parameter at the end of inflation H_{inf} is typically much smaller than m_ϕ in this case:

$$\frac{H_{\text{inf}}}{m_\phi} \simeq \frac{v_\phi}{\sqrt{6}nM_{\text{Pl}}} \ll 1. \quad (6)$$

Using the standard technique to calculate the large-scale curvature perturbation [60], one finds the scalar spectral index and tensor-to-scalar ratio as

$$n_s \simeq 1 - \frac{2}{N} \frac{n-1}{n-2}, \quad r \simeq \frac{16n}{N(n-2)} \left[\frac{1}{2Nn(n-2)} \frac{v_\phi^2}{M_{\text{Pl}}^2} \right]^{\frac{n}{n-2}}, \quad (7)$$

where N is the e-folding number of the cosmic microwave background (CMB) scale, which lies between 50 and 60 depending on the subsequent thermal history. Thus the tensor-to-scalar ratio is negligibly small in small-field models with

³ A pre-inflation before the observed inflation can solve the initial condition problem of the hilltop inflation. If there exist a Hubble induced mass term during the pre-inflation and a small \mathbb{Z}_2 ($\phi \rightarrow -\phi$) breaking term, the initial condition is dynamically selected [59].

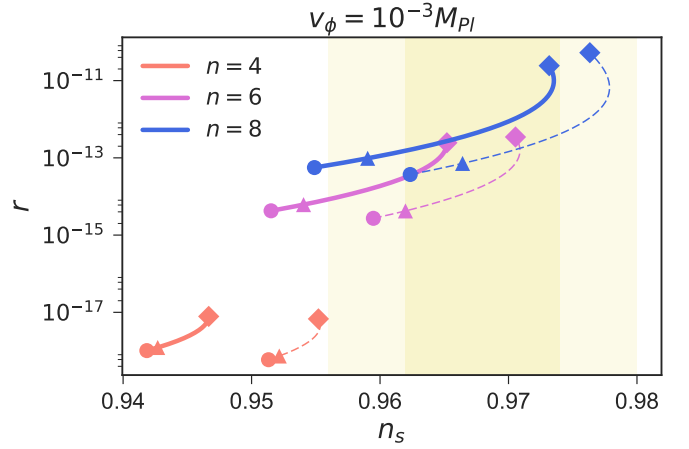


FIG. 1. Here we show n_s - r plane for $n = 4, 6, 8$ with varying k from 10^{-4} to 10^{-2} . The solid (dashed) lines correspond to $N = 50$ (60). The circle, triangle, and square represent points at $k = 10^{-4}, 10^{-3}, 10^{-2}$ respectively. The yellow shaded region stands for one and two sigma regions of n_s [61].

$v_\phi \ll M_{\text{Pl}}$. The overall normalization of the curvature perturbation observed by the Planck satellite [61] implies

$$\mathcal{P}_\zeta \simeq 2.2 \times 10^{-9} \simeq \frac{[2n((n-2)N)^{n-1}]^{\frac{2}{n-2}}}{12\pi^2} \frac{\Lambda^4}{(v_\phi^n M_{\text{Pl}}^{n-4})^{\frac{2}{n-2}}}. \quad (8)$$

It relates Λ and v_ϕ and hence there is essentially one parameter left, which we take v_ϕ hereafter.

For a reasonable value of n , the predicted spectral index [Eq. (7)] is slightly outside the favored range: $n_s = 0.968(6)$ at 68% confidence level [61]. This discrepancy is resolved if there exists the following Planck suppressed operator [55, 56]:

$$\delta V_{\text{Pl}} = -\Lambda^4 \frac{k}{2} \frac{\phi^2}{M_{\text{Pl}}^2}, \quad (9)$$

with $k \lesssim \mathcal{O}(1/nN)$. While it is too small to change the inflaton dynamics significantly, it can shift the slow-roll parameter η for a certain range of k . If $n \geq 6$, it is possible to shift the spectral index within 68% confidence level for $N = 50$ –60. See Fig. 1 and Ref. [62]. Since the suitable value of k is small, this term is safely neglected in the oscillation phase. Thus, we use the potential given in Eq. (4) in the following discussion.

B. Higgs-inflaton couplings and bare mass term

If we denote $\varphi \equiv v_\phi - \phi$, the potential is given as

$$U(\phi, h) = V(v_\phi - \varphi) + \frac{1}{2} \left(m_h^2 + \tilde{\sigma}_{\phi h} v_\phi + \lambda_{\phi h} v_\phi^2 \right) h^2 + \frac{\sigma_{\phi h}}{2} \varphi h^2 + \frac{\lambda_{\phi h}}{2} \varphi^2 h^2 + \frac{\lambda_h}{4} h^4, \quad (10)$$

where we have defined

$$\sigma_{\phi h} \equiv -(\tilde{\sigma}_{\phi h} + 2\lambda_{\phi h} v_\phi). \quad (11)$$

Note that $\varphi = 0$ at the minimum of the potential. Here comes our crucial observation. In order to realize the EW scale, the

bare Higgs mass and the mass coming from the inflaton VEV must be canceled:^{b4}

$$m_h^2 + \tilde{\sigma}_{\phi h} v_\phi + \lambda_{\phi h} v_\phi^2 = 0. \quad (12)$$

It is a tuning, but we cannot avoid it since we assume that the SM is valid up to some high-energy scale aside from the inflaton sector. Thus, the potential is now given by

$$U(\phi, h) = V(v_\phi - \varphi) + \frac{\sigma_{\phi h}}{2} \varphi h^2 + \frac{\lambda_{\phi h}}{2} \varphi^2 h^2 + \frac{\lambda_h}{4} h^4. \quad (13)$$

In particular, the Higgs is almost massless at $\varphi = 0$.

Now we discuss quantum corrections to the potential. The Higgs-inflaton couplings modify/induce runnings of the Higgs four point coupling/inflaton self-interactions. Here let us focus on radiative corrections to the inflaton self-interactions; for the Higgs four point coupling, see the next Sec. II C. As one can infer from Eq. (4), the potential for the low-scale inflation has to be extremely flat, and hence only a small change might spoil the successful inflation. Suppose that the effective potential around the vacuum $\langle \phi \rangle \sim v_\phi$ is given by Eq. (13) at the end of inflation for some renormalization scale μ . We will take μ as the typical scale of the preheating dynamics ($\mu \gtrsim m_\phi$). See Sec. II C for more details. We put bounds on the couplings defined at this scale since we are interested the preheating dynamics. Now the question is whether or not inflaton self-interactions are radiatively induced for $\phi \rightarrow 0$ and spoil the inflation. At the one-loop level, the radiative correction is given by the Coleman-Weinberg effective potential,

$$V_{\text{CW}}(\phi) = \frac{m_h^4(\phi)}{64\pi^2} \ln\left(\frac{m_h^2(\phi)}{\mu^2}\right), \quad (14)$$

where we define $m_h^2(\phi) \equiv m_h^2 + \tilde{\sigma}_{\phi h} \phi + \lambda_{\phi h} \phi^2$, and the couplings are evaluated at the scale μ . We have assumed $m_h^2(\phi) > 0$ during inflation. Otherwise, the Higgs potential might be destabilized during inflation (see Sec. III). In order not to change the tree-level inflaton potential too much during inflation, we need $|\partial V_{\text{CW}}/\partial \phi| \lesssim |\partial V/\partial \phi|$. It roughly indicates

$$|\sigma_{\phi h}| \lesssim m_\phi \left(\frac{v_\phi}{M_{\text{Pl}}}\right)^{\frac{n-1}{n-2}}, \quad |\lambda_{\phi h}| \lesssim \frac{m_\phi}{M_{\text{Pl}}} \left(\frac{v_\phi}{M_{\text{Pl}}}\right)^{\frac{1}{n-2}}, \quad (15)$$

for $\tilde{\sigma}_{\phi h} \neq 0$. For $\tilde{\sigma}_{\phi h} \simeq 0$, we have instead

$$|\sigma_{\phi h}| \lesssim m_\phi \frac{v_\phi}{M_{\text{Pl}}}, \quad |\lambda_{\phi h}| \lesssim \frac{m_\phi}{M_{\text{Pl}}}. \quad (16)$$

C. Higgs potential

Finally, we discuss the Higgs quartic self-coupling λ_h . In order to understand the high-energy behavior of λ_h , we must carefully consider the scalar threshold correction [63, 64]. Once we neglect the Higgs-inflaton quartic coupling, the potential at around the minimum is written as

$$U \simeq \frac{m_\phi^2}{2} \left(\varphi + \frac{\sigma_{\phi h} h^2}{2m_\phi^2} \right)^2 + \frac{1}{4} \left(\lambda_h - \frac{\sigma_{\phi h}^2}{2m_\phi^2} \right) h^4. \quad (17)$$

^{b4} We have neglected the EW scale since we are interested in the phenomena whose energy scale is much higher than the EW scale.

Thus the Higgs potential below the energy scale of m_ϕ is

$$V_{\text{SM}}(h) = \frac{\lambda_{\text{SM}}}{4} h^4, \quad \lambda_{\text{SM}} = \lambda_h - \frac{\sigma_{\phi h}^2}{2m_\phi^2}. \quad (18)$$

It is clear that the quartic coupling λ_{SM} in the low-energy effective theory is different from λ_h .

Up to the energy scale of m_ϕ , the running of λ_{SM} is just that of the SM, and hence it turns to be negative at around 10^{10} GeV according to the current center values of the top/Higgs masses. For simplicity, we approximate it as

$$\lambda_{\text{SM}} = -0.01 \times \text{sgn}(\mu - h_{\text{inst}}) \quad \text{for } \mu < m_\phi, \quad (19)$$

where μ is the energy scale of the system and h_{inst} is the instability scale of the Higgs potential which we take $h_{\text{inst}} = 10^{10}$ GeV. If $m_\phi < h_{\text{inst}}$, λ_h is positive at least up to at around $\mu = h_{\text{inst}}$.^{b5} Thus, to overcome the potential barrier, the Higgs dispersion must be enhanced as large as $\langle h^2 \rangle \gtrsim h_{\text{inst}}^2 > m_\phi^2$. However, such an enhancement requires a large coupling with inflaton which is likely to spoil the flatness of the inflaton potential (see Eq. (15)).^{b6} Therefore in this paper, we concentrate on the opposite case:

$$m_\phi > h_{\text{inst}}. \quad (20)$$

Then, by matching at $\mu = m_\phi$, the boundary condition for λ_h is roughly given as

$$\lambda_h|_{\mu=m_\phi} = -0.01 + \frac{\sigma_{\phi h}^2}{2m_\phi^2} \Big|_{\mu=m_\phi}. \quad (21)$$

If $\sigma_{\phi h}^2/m_\phi^2 \gtrsim 0.01$, it may significantly affect λ_h so that it helps to stabilize the Higgs potential at the high-energy region.^{b7} Thus, there may be another minimum at around $h \simeq m_\phi$ and $\varphi \simeq -\sigma_{\phi h}$ because of Eqs. (17) and (20), and it may affect the dynamics of the Higgs in the early universe.

Instead of being involved in such a complexity, in this paper we simply concentrate on the case

$$\frac{\sigma_{\phi h}^2}{m_\phi^2} \ll 0.01. \quad (22)$$

Then, we may approximate the quartic coupling as

$$\lambda_h = -0.01 \times \text{sgn}(\mu - h_{\text{inst}}). \quad (23)$$

We take the renormalization scale as $\mu = \max(H_{\text{inf}}, h)$ during inflation [32], and $\mu = \max(H, \sqrt{\langle h^2 \rangle})$ during preheating. Here H is the Hubble parameter, and $\langle h^2 \rangle$ is the dispersion of the Higgs field. Actually, as soon as the resonant Higgs production occurs, the dispersion becomes $\langle h^2 \rangle \gtrsim m_\phi^2$, and hence it dominates over the Hubble parameter.

^{b5} The potential can be even absolutely stable depending on $\sigma_{\phi h}^2/m_\phi^2$ and the sign of $\lambda_{\phi h}$ [63, 64].

^{b6} In fact, the hilltop model ($n = 6$) with $m_\phi < h_{\text{inst}} \sim 10^{10}$ GeV cannot have large resonance parameters because of Eq. (40).

^{b7} If $\lambda_{\phi h}$ is negative, the potential may not be absolutely stable anyway, depending on the precise form of $V(\phi)$.

III. HIGGS DYNAMICS DURING INFLATION

Before studying the preheating stage, we summarize the Higgs dynamics during inflation in this section. As studied extensively [26–38], the de-Sitter fluctuation of the Higgs field may lead to the collapse of the vacuum during inflation if the inflation scale is too high. It is instructive to see what happens if the inflation scale is so low that $H_{\text{inf}} \ll h_{\text{inst}}$.

In the present model, since $\phi \ll v_\phi$ during inflation, the Higgs potential during inflation is approximately given by

$$V(h) \simeq \frac{m_h^2}{2} h^2 + \frac{\lambda_h}{4} h^4, \quad (24)$$

where the bare Higgs mass m_h^2 satisfies Eq. (12). There are two possibilities: $m_h^2 < 0$ and $m_h^2 > 0$.

First, let us consider the case of tachyonic Higgs during inflation: $m_h^2 < 0$, or $\tilde{\sigma}_{\phi h} v_\phi + \lambda_{\phi h} v_\phi^2 > 0$. In this case, the parameters must satisfy

$$|\lambda_h| h_{\text{inst}}^2 > |m_h^2|, \quad (25)$$

since otherwise the potential decreases monotonically toward large h and the Higgs may roll down to the deeper minimum during inflation. As long as Eq. (25) is satisfied, the EW vacuum is stable during inflation if the Hubble scale during inflation is low enough, *i.e.*, $H_{\text{inf}} \ll h_{\text{inst}}$. Otherwise, the de-Sitter fluctuation of the Higgs field is too large to stay at the local minimum of the potential.

Next, let us consider the opposite case: $m_h^2 > 0$, or $\tilde{\sigma}_{\phi h} v_\phi + \lambda_{\phi h} v_\phi^2 < 0$. In this case, $h = 0$ is always a local minimum of the potential, and it is stable against the de-Sitter fluctuation if

$$H_{\text{inf}}^2 \ll \max[h_{\text{inst}}^2, m_h^2/|\lambda_h|]. \quad (26)$$

If the condition (25) or (26) is satisfied, the Higgs field effectively stays at around the origin without overshooting the potential barrier due to the de-Sitter fluctuation. However, it does not guarantee the vacuum stability *after* inflation, since the Higgs fluctuation can be resonantly enhanced during the preheating stage as studied in detail in the next section.

IV. INFLATON AND HIGGS DYNAMICS DURING PREHEATING

In this section, we analytically describe the preheating dynamics of our system. We first discuss resonant inflaton production in Sec. IV A. Since the inflaton potential at around the minimum is far from quadratic in the low-scale inflation model, inflaton particles are resonantly produced from the inflaton condensation. In fact, the inflaton particles can be even tachyonic during the preheating epoch. Hence, the inflaton production is so efficient that the backreaction destroys the inflaton condensation within several times of the oscillation. It sets the end of the preheating epoch, and hence sets the upper bound of the time we follow in this paper.

Then we discuss resonant Higgs production in Sec. IV B. There we make use of a crude approximation that the inflaton potential is dominated by the quadratic one. This is because the purpose of this subsection is to understand the Higgs production qualitatively and to make an order of magnitude estimation of the constraints on the couplings. More rigorous analysis is performed numerically in the next section.

A. Inflaton dynamics during tachyonic oscillation

The inflaton oscillation is typically dominated by the flat part of the potential just after inflation, and it causes a so-called tachyonic preheating phenomenon. Below we closely follow the discussion in Ref. [48] concerning the linear regime of the tachyonic preheating. More details are given in App. A.

There are two stages of tachyonic preheating. The first stage is further divided into the epoch between the point $|\eta| = 1$ and $\epsilon = 1$, and the interval between $\epsilon = 1$ and the first passage of $\phi = v_\phi$. Here ϵ and η are the slow-roll parameters: $\epsilon \equiv M_{\text{pl}}^2 (V'/V)^2/2$, $\eta \equiv M_{\text{pl}}^2 V''/V$. The tachyonic growth starts after $|\eta| \gtrsim 1$, where there is a large hierarchy between η and ϵ in low-scale inflation models. Therefore, the tachyonic growth occurs at the plateau regime of the inflaton potential, and the inflaton fluctuation with $k/a \lesssim H_{\text{inf}}$ will develop. While the inflaton is rolling down the potential, higher momentum modes with $H_{\text{inf}} < k/a \lesssim m_\phi$ also experience tachyonic growth, but modes with low k/a ($\lesssim H_{\text{inf}}$) are most enhanced because they have more time to develop. The inflaton fluctuation with such low-momenta at $\phi = v_\phi$ is estimated as⁹⁸

$$\frac{\delta\phi_k(\phi(t) = v_\phi)}{\delta\phi_k(|\eta| = 1)} = \frac{\dot{\phi}(\phi(t) = v_\phi)}{\dot{\phi}(|\eta| = 1)} \sim \left(\frac{M_{\text{pl}}}{v_\phi}\right)^{\frac{n}{n-2}}. \quad (27)$$

Then the condition for the inflaton fluctuation to remain perturbative after the first passage of $\phi(t) = v_\phi$ is $\langle \delta\phi^2 \rangle \lesssim v_\phi^2$, and it leads to

$$\left(\frac{v_\phi}{M_{\text{pl}}}\right)^{1/(n-2)} \gtrsim \frac{\Lambda}{v_\phi}. \quad (28)$$

Using the Planck normalization (8), this translates into $v_\phi/M_{\text{pl}} \gtrsim 10^{-6} - 10^{-5}$ independently of n . Otherwise, even within one inflaton oscillation, the inflaton condensate may be broken, and the subsequent inflaton-Higgs dynamics would be too complicated. To avoid this complexity, we focus on the case of $v_\phi/M_{\text{pl}} \gtrsim 10^{-6} - 10^{-5}$ so that we can reliably discuss the Higgs dynamics in the second stage explained below.

In the second stage, the system goes into tachyonic inflaton oscillation regime. During this stage, the inflaton oscillation is far from harmonic because the most oscillation period is consumed at the flat part of the potential $\phi \ll v_\phi$. After the j -th oscillation of the inflaton, the field value at the lower endpoint is given by

$$\frac{\phi_j}{v_\phi} \simeq \left(\frac{j\sqrt{3}}{2} \frac{v_\phi}{M_{\text{pl}}}\right)^{1/n}. \quad (29)$$

The most enhanced mode during this tachyonic oscillation stage is basically determined by the curvature of the inflaton potential at $\phi = \phi_j$:

$$\frac{k_*}{a} \simeq m_\phi \left(\frac{j v_\phi}{M_{\text{pl}}}\right)^{(n-2)/(2n)}. \quad (30)$$

⁹⁸ More precisely, the inflaton fluctuation $\delta\phi_k$ should be regarded as its gauge-invariant generalization taking account of the scalar metric perturbation (see Ref. [48] for more detail). Also, note that the curvature perturbation on large-scale is conserved since $\delta\phi_k \propto \dot{\phi}$.

It is this mode ($k = k_*$) that is most enhanced through the whole tachyonic preheating process. Note that it is much different from the ordinary broad resonance in which the inflaton oscillates about the quadratic potential. In our case, the fluctuation becomes nonlinear, *i.e.*, $\langle \delta\phi^2 \rangle \sim v_\phi^2$, within several times of oscillation. See App. A for more detail.

In summary, the inflaton fluctuation becomes nonlinear within several times of oscillation due to the tachyonic preheating. To avoid complications arising from the nonlinearity and thermalization as well as possible model dependent discussions, we conservatively require that the vacuum remains stable at least until the inflaton fluctuation becomes nonlinear in this paper. Otherwise, we cannot avoid the catastrophe anyway. Thus, the tachyonic production of the inflaton particles sets the upper bound of the time during which we follow the dynamics in this paper.

B. Higgs dynamics during preheating

Now we are in a position to study the growth of the Higgs field fluctuation during the preheating stage. In this subsection, we crudely approximate the inflaton potential as quadratic, although the actual inflaton potential just after inflation is typically far from quadratic for low-scale inflation models. Nevertheless, it helps us to understand the numerical results in the next section.

The potential of the inflaton and Higgs at the inflaton oscillation phase is

$$U(\phi, h) = \frac{m_\phi^2}{2} \phi^2 + \frac{\lambda_h}{4} h^4 + \frac{\sigma_{\phi h}}{2} \phi h^2 + \frac{\lambda_{\phi h}}{2} \phi^2 h^2. \quad (31)$$

The inflaton potential is approximately taken to be quadratic around the potential minimum. We consider the preheating dynamics of this system, *i.e.*, the resonant Higgs particle production due to the inflaton oscillation.⁹ The linearized equation of motion of the Higgs is

$$\ddot{h}_k + (k^2 + \sigma_{\phi h} \dot{\phi} + \lambda_{\phi h} \phi^2) h_k = 0, \quad (32)$$

where the dot denotes the derivative with respect to the time. We have moved to the momentum space with k being the momentum, and neglected the Hubble expansion because of Eq. (6). The inflaton oscillation is described as

$$\phi = \varphi_{\text{ini}} \cos(m_\phi t), \quad (33)$$

under the quadratic approximation. Here φ_{ini} is the initial inflaton oscillation amplitude, which is roughly $\varphi_{\text{ini}} \sim v_\phi$ (remember that $\varphi \equiv v_\phi - \phi$). Note again that, although the oscillation amplitude is a time-decreasing function due to the Hubble expansion, the Hubble parameter is so small that the effect of Hubble expansion is practically negligible in low-scale inflation models with $H_{\text{inf}} \ll m_\phi$ [Eq. (6)].

By substituting it to Eq. (32), we obtain the Whittaker-Hill equation:

$$h_k'' + [A_k + 2p \cos 2z + 2q \cos 4z] h_k = 0, \quad (34)$$

⁹ The EW vacuum stability of this system during the preheating epoch is studied for large field inflation models in Refs. [42, 44].

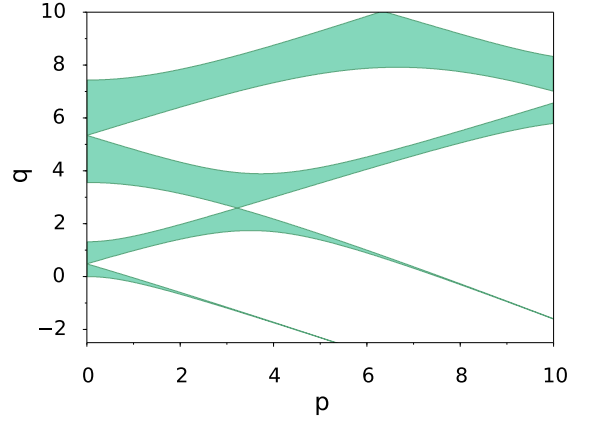


FIG. 2. The stability/instability chart of the Whittaker-Hill equation for the mode with $k = 0$. The green shaded region corresponds to the stability region, while the unshaded region does to the instability region. The chart is even with respect to p .

where

$$A_k \equiv \frac{4k^2}{m_\phi^2} + 2q, \quad p \equiv \frac{2\sigma_{\phi h} \varphi_{\text{ini}}}{m_\phi^2}, \quad q \equiv \frac{\lambda_{\phi h} \varphi_{\text{ini}}^2}{m_\phi^2}, \quad z \equiv \frac{m_\phi t}{2}, \quad (35)$$

and the prime denotes the derivative with respect to z . The term with q leads to the usual parametric resonance [45, 46], while the term with p potentially leads to the tachyonic resonance [65]. In Fig. 2, we show the stability/instability chart of the Whittaker-Hill equation for $k = 0$ for both positive and negative q . If the parameters are in the instability region (the unshaded region), Eq. (34) has exponentially growing solutions, resulting in the resonant Higgs production. A similar stability/instability chart can be drawn for finite k modes. The resonance parameters p and q are useful for estimating the strength of the resonance even for a potential that is far from quadratic, as in the case of the hilltop potential. For more details on the Whittaker-Hill equation and the Floquet theory, see, *e.g.*, Refs. [42, 66] and references therein.

In terms of the resonance parameters, the condition

$$p + 2q \geq 0, \quad (36)$$

is necessary for the Higgs not to be tachyonic during inflation. Although it does not necessarily cause a problem even if the Higgs is tachyonic during inflation as long as Eq. (25) is fulfilled (see Sec. III), we will assume that Eq. (36) holds in the following for simplicity.

Once the resonant Higgs production occurs, it forces the EW vacuum to decay into the deeper minimum [39–42, 44]. This is because the produced Higgs particles induce the following tachyonic mass from the Higgs self-quartic coupling:

$$m_{\text{tac};h}^2 \simeq 3\lambda_h \langle h^2 \rangle, \quad (37)$$

where we have used the mean-field approximation. Note that the dispersion is typically $\langle h^2 \rangle \gtrsim m_\phi^2$ for the resonant particle production, and thus we expect $\lambda_h < 0$ as can be seen from Eqs. (20) and (23).

Thus we can constraint the resonance parameters, or the couplings, by requiring that the EW vacuum is stable during

d	N_g	L	dt	dk
2+1	2048	$1500m_\phi^{-1}$	$5 \times 10^{-3}m_\phi^{-1}$	$4.2 \times 10^{-3}m_\phi$

TABLE I. The parameters of our lattice simulation, where d is the spacetime dimension, N_g is the number of grid in each spatial dimension, L is the size of the lattice, dt is the size of the each time step, $dk \equiv 2\pi/L$ is the resolution of the momentum.

the preheating (or within several times of the inflaton oscillation). The tachyonic resonance is effective if $|p|$ exceeds of order unity (see Fig. 2), so we may require

$$|p| \lesssim \mathcal{O}(1), \quad (38)$$

for the EW vacuum stability during the preheating. We will confirm this expectation by classical lattice simulations [67, 68] with a full hilltop inflaton potential in the next section. Note that Eq. (38) implies that $|q| \lesssim \mathcal{O}(1)$ without any accidental cancellation between $\sigma_{\phi h}$ and $\lambda_{\phi h}$. However, we will also discuss the case $|p| \lesssim \mathcal{O}(1)$ and $|q| \gg \mathcal{O}(1)$ at the end of the next section for the completeness of this paper.^{b10}

V. NUMERICAL SIMULATION

In this section we perform classical lattice simulations to study the EW vacuum stability during the preheating epoch. For concreteness, we take $n = 6$ in the inflaton potential (4). The CMB normalization (8) implies

$$\left(\frac{\Lambda}{M_{\text{Pl}}}\right)^4 \simeq 7 \times 10^{-14} \left(\frac{v_\phi}{M_{\text{Pl}}}\right)^3 \left(\frac{N}{60}\right)^{-5/2}. \quad (39)$$

For example, for $v_\phi/M_{\text{Pl}} = 10^{-3}$, we have $\Lambda/M_{\text{Pl}} \simeq 3 \times 10^{-6}$, $H_{\text{inf}} \simeq 10^7$ GeV and $m_\phi \simeq 2 \times 10^{11}$ GeV. Thus the parameters satisfy $H_{\text{inf}} \ll h_{\text{max}} < m_\phi$, and hence this model is indeed a good example of our general argument in the previous sections. The condition (15) is given in terms of p and q as

$$|p| \lesssim \frac{v_\phi}{m_\phi} \left(\frac{v_\phi}{M_{\text{Pl}}}\right)^{5/4}, \quad |q| \lesssim \frac{v_\phi}{m_\phi} \left(\frac{v_\phi}{M_{\text{Pl}}}\right)^{5/4}. \quad (40)$$

In the present case of $n = 6$, the right-hand sides of these inequalities are larger than unity for $v_\phi/M_{\text{Pl}} \gtrsim 10^{-4}$.

We numerically solved the classical equations of motion derived from the Lagrangian (1) as well as the Friedmann equations. We start to solve the equations when the slow-roll parameter ϵ becomes unity. It corresponds to $\varphi_{\text{ini}} \simeq 0.74v_\phi$ for $v_\phi = 10^{-2}M_{\text{Pl}}$, and $\varphi_{\text{ini}} \simeq 0.84v_\phi$ for $v_\phi = 10^{-3}M_{\text{Pl}}$. We took the initial velocity of the inflaton as zero. We also introduced initial Gaussian fluctuations that mimic the quantum fluctuations for the inflaton and the Higgs. We have assumed that they are in the vacuum state initially. This is justified for $v_\phi/M_{\text{Pl}} \gtrsim 10^{-6} - 10^{-5}$ since we can safely neglect inflaton particle production at the first stage in this case as discussed in Sec. IV A. We have also added h^6 term in the Higgs potential just for numerical convergence. We have checked that it does not modify the dynamics

before the EW vacuum decays. The parameters of our lattice simulations are summarized in Tab. I. For more details on the classical lattice simulation, see for instance Refs. [40, 69, 70] and references therein.

Since we have two different momentum scales (Eq. (30) and m_ϕ), we must take the number of grids N_g to be large. This is why we took the spatial dimension to be two instead of three (see Tab. I). As far as the linear regime is concerned, the results are not expected to change drastically for different numbers of spatial dimensions.

We show our numerical results for $v_\phi = 10^{-2}M_{\text{Pl}}$ and $v_\phi = 10^{-3}M_{\text{Pl}}$ in Figs. 3 and 4 respectively. We have followed the dynamics until $m_\phi t = 150$ and 250 for $v_\phi = 10^{-2}M_{\text{Pl}}$ and $10^{-3}M_{\text{Pl}}$, respectively, since the inflaton condensation is broken slightly before these times. The black line is the inflaton condensation $\langle \varphi \rangle^2$, the red line is the inflaton dispersion $\langle \varphi^2 \rangle - \langle \varphi \rangle^2$, and the blue line is the Higgs dispersion $\langle h^2 \rangle$, where the angle brackets denote the spatial average. They are normalized by the initial amplitude of the inflaton condensation φ_{ini}^2 . The resonance parameters p and q are written at the tops of these figures.

Let us start with the upper panels in Figs. 3 and 4. There, the resonance parameter p satisfies $p \gtrsim \mathcal{O}(1)$, and both $q > 0$ and $q < 0$ cases are considered. As we can see from the figures, the EW vacuum is actually destabilized during the preheating for these cases. On the other hand, we have taken the resonance parameters as $p = q \lesssim \mathcal{O}(1)$ in the lower left panels in Figs. 3 and 4. In these cases, the EW vacuum survives the preheating. Thus the numerical results are consistent with our expectation in Sec. IV B. That is,

$$|p| = \frac{2\sigma_{\phi h}\varphi_{\text{ini}}}{m_\phi^2} \lesssim \mathcal{O}(1), \quad (41)$$

is required for the stability of the EW vacuum during the preheating. We have checked that this criterion is indeed satisfied for several other values of p and q . In particular, we have also calculated the case $p < 0$. In this case, the Higgs becomes tachyonic in the region $\varphi > 0$, where it takes more time for the inflaton to oscillate. Hence the Higgs is more likely to be enhanced and the EW vacuum decays faster compared to the case $p > 0$.^{b11} In any case, the EW vacuum is stable during the preheating as long as Eq. (41) holds and $|q| \sim |p|$. The bound (41) does not strongly depend on v_ϕ since it is expressed solely by the resonance parameters. It is consistent with the numerical results with two different values of v_ϕ .

Eq. (41) is our main result in this paper, and it also implies $|q| \lesssim \mathcal{O}(1)$ if there is no tuning of the parameters. Still, we have also considered the case $|p| \ll q$ for the completeness of our study. Note again that an accidental cancellation between $\sigma_{\phi h}$ and $\lambda_{\phi h}$ is necessary to achieve $q \gg \mathcal{O}(1)$ while satisfying Eq. (41) (see the footnote b10). In this case, the situation is more complicated. When the parametric resonance is dominant, the condition for the EW vacuum destabilization in the linear regime is estimated as [40, 42]^{b12}

$$|\lambda_h| \langle h^2 \rangle \gtrsim k_h^2, \quad (42)$$

^{b11} Note that the trilinear coupling eventually dominates over the quartic coupling as the inflaton approaches to the minimum of its potential.

^{b12} Apparently, the condition, $|\lambda_h \langle h^2 \rangle| \lesssim k_h^2$, does not guarantee the stability for the homogeneous mode of the Higgs, but actually it does. We briefly explain the reason below. See Ref. [40] for the original argument. As can be seen from

^{b10} Note that $q \gtrsim -\mathcal{O}(1)$ from Eqs. (36) and (38).

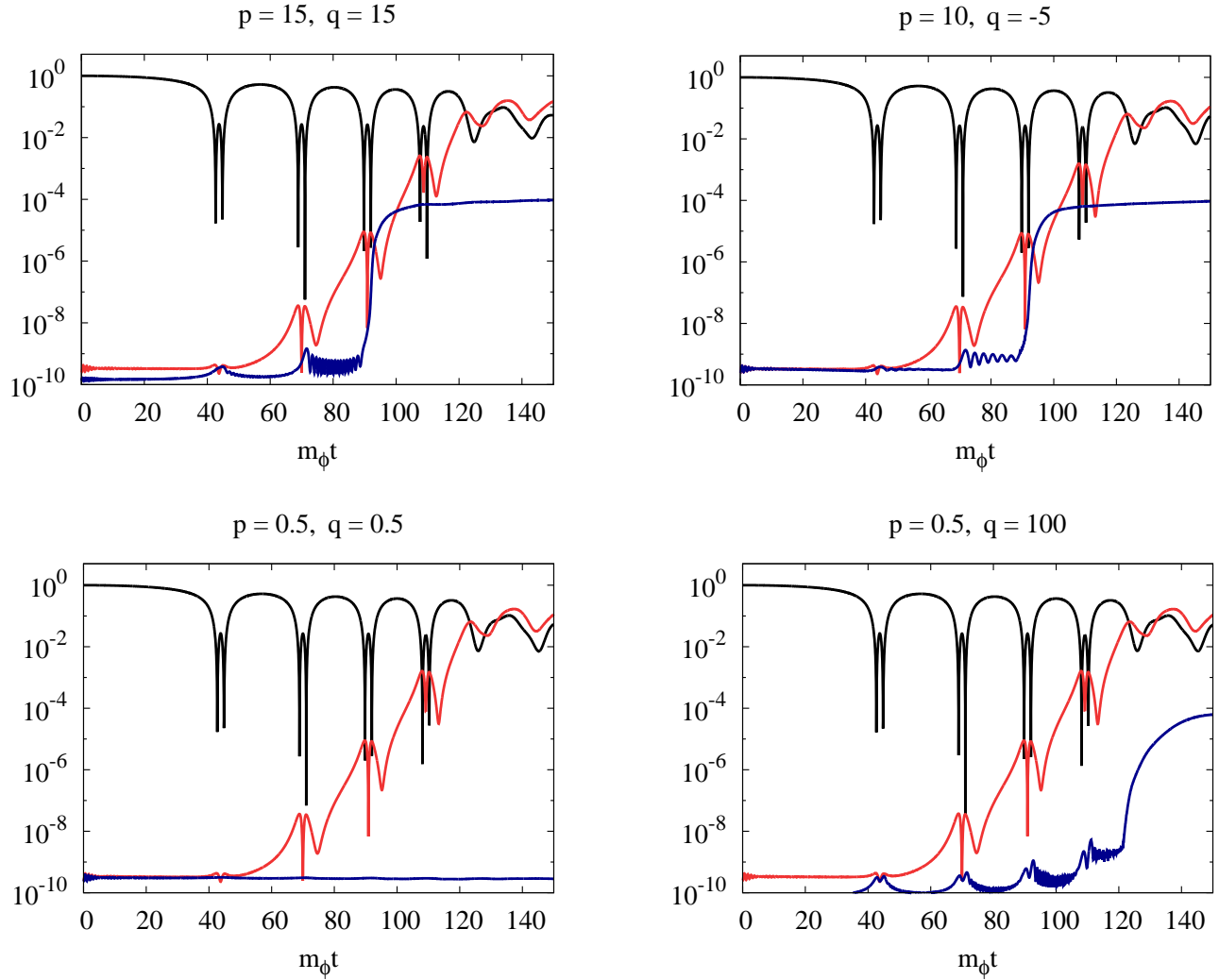


FIG. 3. The time evolution of the inflaton and the Higgs for $v_\phi = 10^{-2} M_{\text{Pl}}$ up to $m_\phi t = 150$. The black line is the inflaton condensation $\langle \varphi^2 \rangle$, the red line is the inflaton two point function $\langle \varphi^2 \rangle - \langle \varphi \rangle^2$ and the blue line is the Higgs two point function $\langle h^2 \rangle$, where the angle brackets denote the spatial average. They are normalized by the initial inflaton amplitude φ_{ini} . The EW vacuum is stable for $(p, q) = (0.5, 0.5)$, while it is destabilized during the preheating for the other cases. The lower right panel corresponds to the case with an accidental cancellation between $\sigma_{\phi h}$ and $\lambda_{\phi h}$.

where $k_h \equiv m_\phi q^{1/4}$ is the typical momentum of the produced Higgs particles. The dispersion grows like $\langle h^2 \rangle \sim k_h^2 e^{\mu_g m_\phi t}$ and the growth factor μ_g does not much depend on q for the parametric resonance [46]. Hence the value of q is not so important in this condition. As a result, it is likely that the EW vacuum does not decay during the linear regime even if we take q to be larger, since we have restricted the number of times of the inflaton oscillations in our analysis (only several times) to avoid complications associated with the nonlinear behavior of the inflaton. However, as the inflaton fluctuations grow and become nonlinear, they can also produce the Higgs particles through the scatterings. It corresponds to the beginning of

the thermalization, which is studied in detail in, e.g., Ref. [71]. In this regime, the variance of the fields interacting with each other tends to converge to a similar value though the scattering. Therefore, as q (or $\lambda_{\phi h}$) becomes larger, the variance of the Higgs particles $\langle h^2 \rangle$ approaches to that of the inflaton $\langle \varphi^2 \rangle$ faster. In the present case, it might destabilize the EW vacuum since $|\lambda_h| \gg \lambda_{\phi h}$. Actually, in the lower right panels in Figs. 3 and 4, the EW vacuum is destabilized at almost the same time as the system becomes nonlinear for $q \gtrsim \mathcal{O}(10)$. Thus, it might be expected that

$$q = \frac{\lambda_{\phi h} \varphi_{\text{ini}}^2}{m_\phi^2} \lesssim \mathcal{O}(10) \quad \text{if} \quad |p| \lesssim \mathcal{O}(1), \quad (43)$$

is at least required for the stability of the EW vacuum during and also after the preheating.

If we follow the thermalization process for a longer time, the constraints may become tighter than Eqs. (41) and (43). In this sense, Eqs. (41) and (43) are just necessary conditions, and we must also follow the dynamics after the preheating to determine an ultimate fate of the EW vacuum. However, to address

Eq. (34), the Higgs acquires a positive mass term from the Higgs-inflaton coupling. The Higgs escapes from its origin only when the tachyonic mass, $|\delta m_{\text{tach}}^2|$, overcomes the Higgs inflaton coupling. Expanding the effective Higgs mass around $\phi = v_\phi$, one can estimate the time interval, δt , during which $|\delta m_{\text{tach}}^2| \gtrsim m_h^2(\phi)$ as $|\delta m_{\text{tach}}^2| \sim q m_\phi^4 \delta t^2$. If the tachyonic mass term significantly drives the Higgs field during this time interval, or $|\delta m_{\text{tach}}^2| \delta t \gtrsim 1$, the vacuum decay takes place. This requirement coincides with Eq. (42).

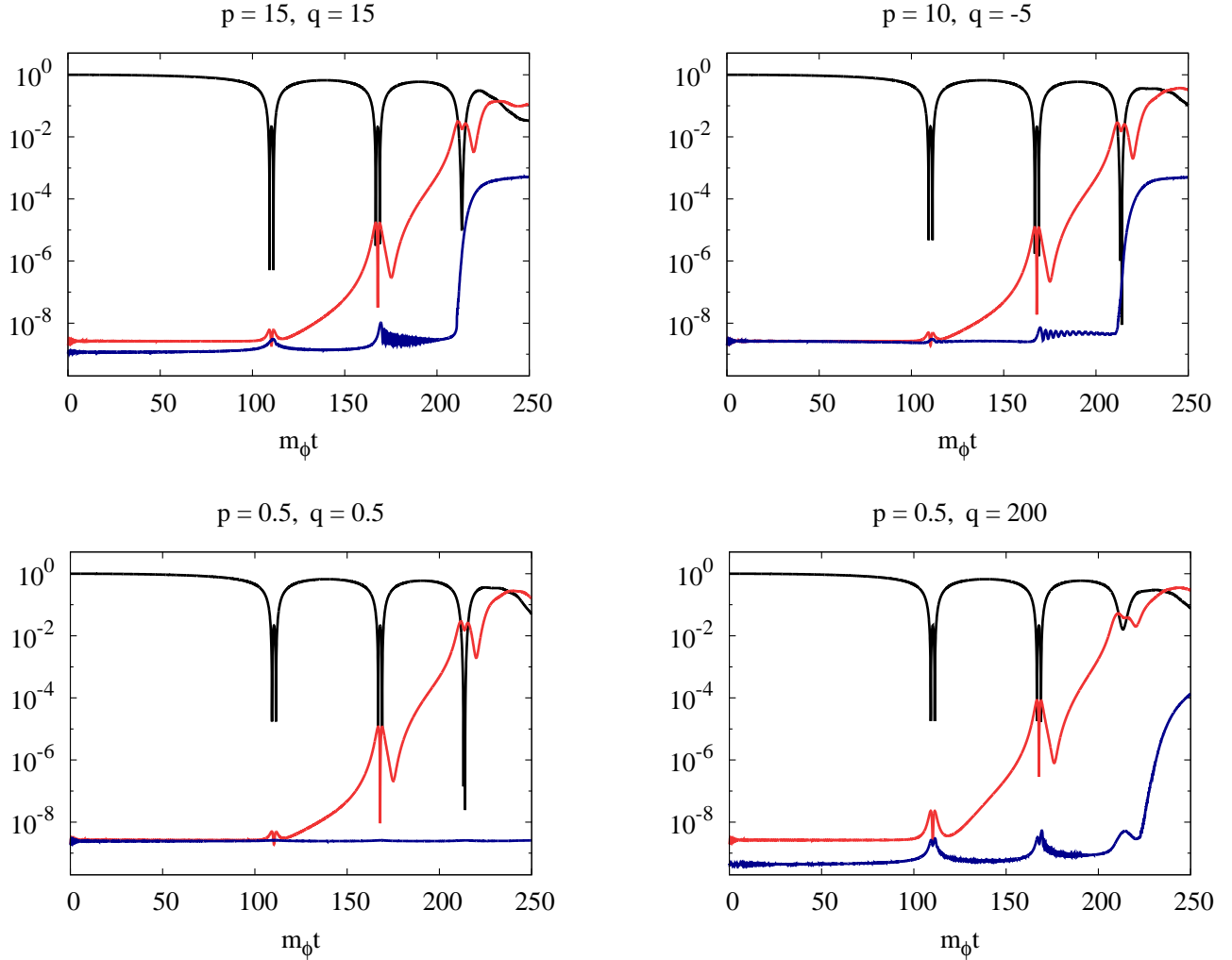


FIG. 4. The time evolution of the inflaton and Higgs for $v_\phi = 10^{-3} M_{\text{Pl}}$ up to $m_\phi t = 250$. The black line is the inflaton condensation $\langle \varphi^2 \rangle$, the red line is the inflaton two point function $\langle \varphi^2 \rangle - \langle \varphi \rangle^2$ and the blue line is the Higgs two point function $\langle h^2 \rangle$, where the angle brackets denote the spatial average. They are normalized by the initial inflaton amplitude φ_{ini} . The EW vacuum is stable for $(p, q) = (0.5, 0.5)$, while it is destabilized during the preheating for the other cases. The lower right panel corresponds to the case with an accidental cancellation between $\sigma_{\phi h}$ and $\lambda_{\phi h}$.

this issue, we should take into account the couplings between the Higgs and the SM particles, which might stabilize the EW vacuum. We leave such a study for future work.

VI. SUMMARY AND DISCUSSIONS

In this paper, we have studied the implications of the EW vacuum metastability during the preheating epoch with low-scale inflation models, taking a hilltop inflation model as an example. We have shown that, although the EW vacuum is naturally stable during inflation for low-scale inflation models, it may decay into the deeper minimum during the preheating epoch due to the resonant Higgs production.

One of the particular features of the hilltop inflation model is that there is a tachyonic preheating in the inflaton sector itself, which is so strong that the inflaton fluctuation becomes nonlinear within several inflaton oscillations. To avoid complications arising from the nonlinearity of the inflaton, we derive necessary conditions of the resonance parameters as $|p| \lesssim \mathcal{O}(1)$ and $q \lesssim \mathcal{O}(10)$ by requiring that the vacuum remains stable un-

til the inflaton becomes nonlinear (see Eq. (35) for the definitions of p and q). However, we also find that even after the inflaton field becomes completely inhomogeneous, thermalization processes between the inflaton and Higgs tend to enhance the Higgs fluctuation, which might cause the EW vacuum decay. In addition to that, the production of other SM particles may also become relevant for such a long time scale, whose effects are unclear. We did not give concrete bound taking into account such effects due to the complexity of the system and limitation of the numerical simulation. In this sense, the bounds we derived should be regarded as just a necessary condition.

Still it might be possible to estimate *sufficient* conditions on the Higgs-inflaton couplings to avoid the EW vacuum decay. If the couplings are small enough ($|p|, |q| \ll 1$), the band width of the Higgs resonance becomes narrow [72–74] and the Hubble expansion can kill the resonant Higgs production. The condition that the narrow resonance does not happen is written as [46],

$$p^2, q^2 \lesssim \frac{H_{\text{inf}}}{m_\phi} \sim \frac{v_\phi}{M_{\text{Pl}}}. \quad (44)$$

If it is satisfied, the only way to produce Higgs bosons is the ordinary perturbative decay/annihilation of the inflaton (without Bose enhancement). The perturbative decay/annihilation rate may be estimated as

$$\Gamma(\varphi \rightarrow hh) \simeq \frac{\sigma_{\phi h}^2}{32\pi m_\phi}, \quad \Gamma(\varphi\varphi \rightarrow hh) \sim \frac{\lambda_{\phi h}^2 \langle \varphi^2 \rangle}{32\pi m_\phi}. \quad (45)$$

One may estimate the conservative bound which is free from the uncertainty of thermalization, by requiring that the Higgs dispersion from the perturbative decay/annihilation never exceeds the instability scale, $\langle h^2 \rangle < h_{\text{inst}}^2$:

$$p^2, q^2 \lesssim \mathcal{O}(10^2) \frac{v_\phi}{M_{\text{Pl}}} \frac{h_{\text{inst}}^2}{m_\phi^2}. \quad (46)$$

While the bounds (46) might be too conservative, it should be noted that we need to take account of the whole thermalization process including gauge bosons and quarks in order to derive more precise bounds.

There are few remarks. First, we would like to comment on possible interactions between the Higgs and the inflaton that are not taken into account in the main text. Although it is higher dimensional, the following term can be large for it respects the shift symmetry of inflaton:

$$\delta \mathcal{L}_{\text{kin}} = c_{\text{kin}} \frac{h^2}{M_{\text{Pl}}^2} (\partial \phi)^2. \quad (47)$$

It induces an oscillating Higgs effective mass during the preheating, and hence excites the Higgs fluctuations. If we use the crude approximation that the inflaton potential is quadratic around the minimum, this coupling contributes to A and q in addition to $\lambda_{\phi h}$, making them independent even for the mode $k=0$. By requiring again Eq. (43), we roughly estimate the constraint as

$$|c_{\text{kin}}| \lesssim \mathcal{O}(10) \times \frac{M_{\text{Pl}}^2}{v_\phi^2}. \quad (48)$$

In Ref. [44], it is found that the resonance can be suppressed by making the ratio A/q to be larger. However, in the present case, the inflaton potential is actually far from quadratic just after inflation, and hence it might be difficult to cancel the oscillating part between $\dot{\varphi}^2$ and φ^2 . A similar discussion can be applied for the Higgs-gravity non-minimal coupling $\xi_h h^2 R$.

The next one is the possibility that the Higgs mass at $\varphi=0$ in the early universe is different from that in the present universe. It is possible if, for instance, the Higgs couples to a scalar field χ other than the inflaton which has a finite VEV in the early universe. The cancellation (12) does not hold in this case, and the resonance due to the inflaton oscillation can be suppressed if the Higgs mass at $\varphi=0$ is larger than of order m_ϕ . However, χ must relax to its potential minimum at some epoch so that the Higgs mass is of the order of the EW scale in the present universe. We may need to discuss the resonant Higgs production during such a relaxation of χ instead, if the mass of χ is larger than the instability scale of the EW vacuum.

Third, we comment on other low-scale inflation models. While there are various class of low-scale inflation models, we expect that the bounds we found ($|p| \lesssim \mathcal{O}(1)$ and $|q| \lesssim \mathcal{O}(10)$) do not change much. This is because our bounds only depend

on the form of the Higgs-inflaton potential around the minimum (31). Thus they may be applied to other low-scale models *e.g.*, hybrid inflation [75] and attractor inflation [76], although more detailed study is needed to rigorously confirm it.

Finally, we again stress that, it is still far from clear in what condition the EW vacuum is stable from the end of the preheating to the end of the thermalization process. On the one hand, the EW vacuum stability during inflation and preheating is studied in detail in this paper as well as the previous literature [26–44]. On the other hand, it is known that the lifetime of the EW vacuum is long enough once the system is completely thermalized [26, 77]. However, we are still lacking studies on the EW vacuum (in)stability from the end of the preheating to the end of the thermalization. Just after the preheating, the momentum distribution of the Higgs (as well as the other SM particles) is far from the thermal equilibrium, and it evolves with time due to the scatterings while approaching to the thermal equilibrium. It is possible that the EW vacuum decay is activated during this thermalization process depending on the shape of the momentum distribution. For instance, if the Higgs modes become larger than other SM particles at some time, the vacuum decay can be enhanced; the resonant particle production studied in this paper may be viewed as an extreme example of this situation. Thus, it is expected that the fate of our vacuum strongly depends on the detailed thermalization process. This issue is worth investigating in detail since we cannot avoid discussions on this point to determine an ultimate fate of the EW vacuum. Hopefully we will come back to this issue in future publication.

ACKNOWLEDGMENTS

This work was supported in part by the JSPS Research Fellowships for Young Scientists (YE and KM) and the Program for Leading Graduate Schools, MEXT, Japan (YE). This work was also supported by the Grant-in-Aid for Scientific Research on Scientific Research A (No.26247042 [KN]), Young Scientists B (No.26800121 [KN]) and Innovative Areas (No.26104009 [KN], No.15H05888 [KN]).

Appendix A: Tachyonic preheating after hilltop inflation

In this Appendix, we summarize the properties of tachyonic preheating during the inflaton oscillation after hilltop inflation. The most discussion below follows Ref. [48].

Let us denote by ϕ_j the lower endpoint field value of the inflaton after j -th inflaton oscillation and t_j the time at which $\phi = \phi_j$. The endpoint is evaluated from the energy conservation:

$$V(\phi_j) - V(\phi_{j+1}) = \int_{t_j}^{t_{j+1}} dt 3H \dot{\phi}^2 = \int_{\phi_j}^{\phi_{j+1}} d\phi 3H \dot{\phi}. \quad (A1)$$

The integral is dominated around the potential minimum where $\dot{\phi} \sim v$ and $|\phi| \sim \Lambda^2$. Thus we obtain

$$\frac{\phi_j}{v_\phi} \sim \left(\frac{j\sqrt{3}}{2} \frac{v_\phi}{M_{\text{Pl}}} \right)^{1/n}. \quad (A2)$$

Note that $\phi_{j=1} > \phi_{\text{end}}^{(\epsilon)}$, where $\phi_{\text{end}}^{(\epsilon)}/v_\phi \sim (v_\phi/M_{\text{Pl}})^{1/(n-1)}$ denotes the field value at $\epsilon=1$. The time period of j -th oscillation is given by

$$t_{j+1} - t_j \sim \frac{1}{m_\phi} \left(\frac{v_\phi}{\phi_j} \right)^{(n-2)/2}, \quad (A3)$$

hence it is much longer than the inverse of the mass scale around the potential minimum, as clearly seen in Figs. 3-4.

We consider the growth of the inflaton fluctuation $\delta\phi_k$ with a wavenumber k in the linear approximation during $j+1$ oscillation: $t_j \leq t \leq t_{j+1}$. Below, we neglect the Hubble expansion since all the time scales are much shorter than the Hubble time scale and take the scale factor $a = 1$ for notational simplicity. We further divide the one oscillation into three phases: (a) $t_j < t < t_m^-$, (b) $t_m^- < t < t_m^+$, (c) $t_m^+ < t < t_{j+1}$, where t_m^\pm denotes the time when ϕ passes through ϕ_m , the field value at which V'' takes negative maximum value:

$$\frac{\phi_m}{v_\phi} = \left(\frac{n-2}{2(2n-1)} \right)^{1/n}. \quad (\text{A4})$$

First, in the stage (a), modes with $k \lesssim m_\phi$ experience tachyonic instability within the field range $\phi_{\text{tac}} \leq \phi < \phi_m$, where ϕ_{tac} at which the mode begins to be tachyonic:

$$\frac{\phi_{\text{tac}}}{v_\phi} \simeq \frac{\phi_j}{v_\phi} \times \max \left[1, \left(\frac{k}{k_*} \right)^{2/(n-2)} \right], \quad (\text{A5})$$

with $k_* \sim m_\phi (j v_\phi / M_P)^{(n-2)/(2n)}$ corresponding to the tachyonic mass scale around $\phi = \phi_j$. Then the inflaton fluctuation $\delta\phi_k$ is enhanced by an exponential factor e^{X_k} with

$$X_k = \int_{\phi_{\text{tac}}}^{\phi_m} \frac{\sqrt{|V''+k^2|}}{\dot{\phi}} d\phi \sim \sqrt{\frac{n(n-1)}{2}} \log \left(\frac{\phi_m}{\phi_{\text{tac}}} \right). \quad (\text{A6})$$

However, it should be noticed that the same mode also experiences exponential decay in the third stage (c). It is easy to imagine that in the limit of $k \rightarrow 0$ this exponential decay during the stage (c) exactly cancels the exponential growth during the stage (a), because it is just the same as the dynamics of the homogeneous mode. For finite k , however, there is a phase shift during the stage (b), which causes a

mismatch between the growing solution in the stage (a) and the decaying solution in the stage (c). Schematically, the phase of $\delta\phi_k$ is rotated during the stage (b) as

$$e^{i\sqrt{m_\phi^2+k^2}t} \sim e^{im_\phi t} \left(1 + i \frac{k^2}{m_\phi^2} \right), \quad (\text{A7})$$

where we used $k \ll m_\phi$ and $t \sim t_m^+ - t_m^- \sim m_\phi^{-1}$. Therefore, a small fraction of k^2/m_ϕ^2 at the end of stage (b) connects to the growing mode in the stage (c). The net enhancement factor in one oscillation is then estimated as

$$F_k \equiv \left| \frac{\delta\phi_k(t_{j+1})}{\delta\phi_k(t_j)} \right| \sim \left| 1 + i \frac{k^2}{m_\phi^2} e^{2X_k} \right|. \quad (\text{A8})$$

Using (A6), it is found that F_k is peaked around $k \simeq k_*$, where we have

$$F_{k_*} \sim \left(\frac{m_\phi^2}{k_*^2} \right)^{x_n-1}, \quad x_n \equiv \frac{\sqrt{2n(n-1)}}{n-2}. \quad (\text{A9})$$

Note that it is much larger than unity, hence the inflaton fluctuation is enhanced by orders of magnitude within one oscillation for $v_\phi \ll M_{\text{Pl}}$. This is much different from the ordinary preheating with the parametric resonance.

The variance of the field fluctuation after the j -th inflaton oscillation is now dominated by the modes $k \sim k_*$ and estimated as

$$\langle \delta\phi^2 \rangle \sim k_*^2 (F_{k_*})^{2j} \sim m_\phi^2 \left(\frac{M_P}{v_\phi} \right)^{\frac{n-2}{n} [2j(x_n-1)-1]}. \quad (\text{A10})$$

It is true if $x_n > 3/2$ which is valid for $n < 27$. Thus it will take only a few or several inflaton oscillations for the fluctuation to become nonlinear for low-scale inflation $v_\phi \ll M_{\text{Pl}}$.

-
- [1] M. Sher, *Phys. Rept.* **179**, 273 (1989).
[2] P. B. Arnold, *Phys. Rev.* **D40**, 613 (1989).
[3] G. W. Anderson, *Phys. Lett.* **B243**, 265 (1990).
[4] P. B. Arnold and S. Vokos, *Phys. Rev.* **D44**, 3620 (1991).
[5] J. R. Espinosa and M. Quiros, *Phys. Lett.* **B353**, 257 (1995), [arXiv:hep-ph/9504241 \[hep-ph\]](#).
[6] G. Isidori, G. Ridolfi, and A. Strumia, *Nucl. Phys.* **B609**, 387 (2001), [arXiv:hep-ph/0104016 \[hep-ph\]](#).
[7] J. Ellis, J. R. Espinosa, G. F. Giudice, A. Hoecker, and A. Riotto, *Phys. Lett.* **B679**, 369 (2009), [arXiv:0906.0954 \[hep-ph\]](#).
[8] F. Bezrukov and M. Shaposhnikov, *JHEP* **07**, 089 (2009), [arXiv:0904.1537 \[hep-ph\]](#).
[9] J. Elias-Miro, J. R. Espinosa, G. F. Giudice, G. Isidori, A. Riotto, and A. Strumia, *Phys. Lett.* **B709**, 222 (2012), [arXiv:1112.3022 \[hep-ph\]](#).
[10] F. Bezrukov, M. Yu. Kalmykov, B. A. Kniehl, and M. Shaposhnikov, *JHEP* **10**, 140 (2012), [arXiv:1205.2893 \[hep-ph\]](#).
[11] G. Degrassi, S. Di Vita, J. Elias-Miro, J. R. Espinosa, G. F. Giudice, G. Isidori, and A. Strumia, *JHEP* **08**, 098 (2012), [arXiv:1205.6497 \[hep-ph\]](#).
[12] I. Masina, *Phys. Rev.* **D87**, 053001 (2013), [arXiv:1209.0393 \[hep-ph\]](#).
[13] D. Buttazzo, G. Degrassi, P. P. Giardino, G. F. Giudice, F. Sala, A. Salvio, and A. Strumia, *JHEP* **12**, 089 (2013), [arXiv:1307.3536 \[hep-ph\]](#).
[14] A. V. Bednyakov, B. A. Kniehl, A. F. Pikelner, and O. L. Veretin, *Phys. Rev. Lett.* **115**, 201802 (2015), [arXiv:1507.08833 \[hep-ph\]](#).
[15] G. Isidori, V. S. Rychkov, A. Strumia, and N. Tetradis, *Phys. Rev.* **D77**, 025034 (2008), [arXiv:0712.0242 \[hep-ph\]](#).
[16] V. Branchina, E. Messina, and D. Zappala, *Europhys. Lett.* **116**, 21001 (2016), [arXiv:1601.06963 \[hep-ph\]](#).
[17] A. Rajantie and S. Stopyra, *Phys. Rev.* **D95**, 025008 (2017), [arXiv:1606.00849 \[hep-th\]](#).
[18] A. Salvio, A. Strumia, N. Tetradis, and A. Urbano, *JHEP* **09**, 054 (2016), [arXiv:1608.02555 \[hep-ph\]](#).
[19] P. Burda, R. Gregory, and I. Moss, *Phys. Rev. Lett.* **115**, 071303 (2015), [arXiv:1501.04937 \[hep-th\]](#).
[20] B. Grinstein and C. W. Murphy, *JHEP* **12**, 063 (2015), [arXiv:1509.05405 \[hep-ph\]](#).
[21] P. Burda, R. Gregory, and I. Moss, *JHEP* **06**, 025 (2016), [arXiv:1601.02152 \[hep-th\]](#).
[22] N. Tetradis, *JCAP* **1609**, 036 (2016), [arXiv:1606.04018 \[hep-ph\]](#).
[23] D. Gorbunov, D. Levkov, and A. Panin, (2017), [arXiv:1704.05399 \[astro-ph.CO\]](#).
[24] D. Canko, I. Gialamas, G. Jelic-Cizmek, A. Riotto, and N. Tetradis, (2017), [arXiv:1706.01364 \[hep-th\]](#).
[25] K. Mukaida and M. Yamada, (2017), [arXiv:1706.04523 \[hep-th\]](#).
[26] J. R. Espinosa, G. F. Giudice, and A. Riotto, *JCAP* **0805**, 002 (2008), [arXiv:0710.2484 \[hep-ph\]](#).
[27] O. Lebedev and A. Westphal, *Phys. Lett.* **B719**, 415 (2013), [arXiv:1210.6987 \[hep-ph\]](#).
[28] A. Kobakhidze and A. Spencer-Smith, *Phys. Lett.* **B722**, 130 (2013), [arXiv:1301.2846 \[hep-ph\]](#).
[29] M. Fairbairn and R. Hogan, *Phys. Rev. Lett.* **112**, 201801 (2014), [arXiv:1403.6786 \[hep-ph\]](#).
[30] K. Enqvist, T. Meriniemi, and S. Nurmi, *JCAP* **1407**, 025 (2014), [arXiv:1404.3699 \[hep-ph\]](#).
[31] A. Hook, J. Kearney, B. Shakya, and K. M. Zurek, *JHEP* **01**, 061

- (2015), arXiv:1404.5953 [hep-ph].
- [32] M. Herranen, T. Markkanen, S. Nurmi, and A. Rajantie, *Phys. Rev. Lett.* **113**, 211102 (2014), arXiv:1407.3141 [hep-ph].
- [33] K. Kamada, *Phys. Lett.* **B742**, 126 (2015), arXiv:1409.5078 [hep-ph].
- [34] A. Shkerin and S. Sibiryakov, *Phys. Lett.* **B746**, 257 (2015), arXiv:1503.02586 [hep-ph].
- [35] J. Kearney, H. Yoo, and K. M. Zurek, *Phys. Rev.* **D91**, 123537 (2015), arXiv:1503.05193 [hep-th].
- [36] J. R. Espinosa, G. F. Giudice, E. Morgante, A. Riotto, L. Senatore, A. Strumia, and N. Tetradis, *JHEP* **09**, 174 (2015), arXiv:1505.04825 [hep-ph].
- [37] W. E. East, J. Kearney, B. Shakya, H. Yoo, and K. M. Zurek, *Phys. Rev.* **D95**, 023526 (2017), [Phys. Rev.D95,023526(2017)], arXiv:1607.00381 [hep-ph].
- [38] A. Joti, A. Katsis, D. Loupas, A. Salvio, A. Strumia, N. Tetradis, and A. Urbano, (2017), arXiv:1706.00792 [hep-ph].
- [39] M. Herranen, T. Markkanen, S. Nurmi, and A. Rajantie, *Phys. Rev. Lett.* **115**, 241301 (2015), arXiv:1506.04065 [hep-ph].
- [40] Y. Ema, K. Mukaida, and K. Nakayama, *JCAP* **1610**, 043 (2016), arXiv:1602.00483 [hep-ph].
- [41] K. Kohri and H. Matsui, *Phys. Rev.* **D94**, 103509 (2016), arXiv:1602.02100 [hep-ph].
- [42] K. Enqvist, M. Karciauskas, O. Lebedev, S. Rusak, and M. Zatta, *JCAP* **1611**, 025 (2016), arXiv:1608.08848 [hep-ph].
- [43] M. Postma and J. van de Vis, *JCAP* **1705**, 004 (2017), arXiv:1702.07636 [hep-ph].
- [44] Y. Ema, M. Karciauskas, O. Lebedev, and M. Zatta, (2017), arXiv:1703.04681 [hep-ph].
- [45] L. Kofman, A. D. Linde, and A. A. Starobinsky, *Phys. Rev. Lett.* **73**, 3195 (1994), arXiv:hep-th/9405187 [hep-th].
- [46] L. Kofman, A. D. Linde, and A. A. Starobinsky, *Phys. Rev.* **D56**, 3258 (1997), arXiv:hep-ph/9704452 [hep-ph].
- [47] M. Desroche, G. N. Felder, J. M. Kratochvil, and A. D. Linde, *Phys. Rev.* **D71**, 103516 (2005), arXiv:hep-th/0501080 [hep-th].
- [48] P. Brax, J.-F. Dufaux, and S. Mariadassou, *Phys. Rev.* **D83**, 103510 (2011), arXiv:1012.4656 [hep-th].
- [49] S. Antusch, D. Nolde, and S. Orani, *JCAP* **1506**, 009 (2015), arXiv:1503.06075 [hep-ph].
- [50] S. Antusch, F. Cefala, D. Nolde, and S. Orani, *JCAP* **1602**, 044 (2016), arXiv:1510.04856 [hep-ph].
- [51] A. D. Linde, *Second Seminar on Quantum Gravity Moscow, USSR, October 13-15, 1981*, *Phys. Lett.* **B108**, 389 (1982).
- [52] A. Albrecht and P. J. Steinhardt, *Phys. Rev. Lett.* **48**, 1220 (1982).
- [53] G. Barenboim, E. J. Chun, and H. M. Lee, *Phys. Lett.* **B730**, 81 (2014), arXiv:1309.1695 [hep-ph].
- [54] L. Boubekeur and D. Lyth, *JCAP* **0507**, 010 (2005), arXiv:hep-ph/0502047 [hep-ph].
- [55] K. Kumekawa, T. Moroi, and T. Yanagida, *Prog. Theor. Phys.* **92**, 437 (1994), arXiv:hep-ph/9405337 [hep-ph].
- [56] K. I. Izawa and T. Yanagida, *Phys. Lett.* **B393**, 331 (1997), arXiv:hep-ph/9608359 [hep-ph].
- [57] T. Asaka, K. Hamaguchi, M. Kawasaki, and T. Yanagida, *Phys. Rev.* **D61**, 083512 (2000), arXiv:hep-ph/9907559 [hep-ph].
- [58] V. N. Senoguz and Q. Shafi, *Phys. Lett.* **B596**, 8 (2004), arXiv:hep-ph/0403294 [hep-ph].
- [59] K. I. Izawa, M. Kawasaki, and T. Yanagida, *Phys. Lett.* **B411**, 249 (1997), arXiv:hep-ph/9707201 [hep-ph].
- [60] A. R. Liddle and D. H. Lyth, *Cosmological inflation and large scale structure* (2000).
- [61] P. A. R. Ade *et al.* (Planck), *Astron. Astrophys.* **594**, A20 (2016), arXiv:1502.02114 [astro-ph.CO].
- [62] K. Nakayama and F. Takahashi, *JCAP* **1205**, 035 (2012), arXiv:1203.0323 [hep-ph].
- [63] O. Lebedev, *Eur. Phys. J.* **C72**, 2058 (2012), arXiv:1203.0156 [hep-ph].
- [64] J. Elias-Miro, J. R. Espinosa, G. F. Giudice, H. M. Lee, and A. Strumia, *JHEP* **06**, 031 (2012), arXiv:1203.0237 [hep-ph].
- [65] J. F. Dufaux, G. N. Felder, L. Kofman, M. Peloso, and D. Podolsky, *JCAP* **0607**, 006 (2006), arXiv:hep-ph/0602144 [hep-ph].
- [66] J. Lachapelle and R. H. Brandenberger, *JCAP* **0904**, 020 (2009), arXiv:0808.0936 [hep-th].
- [67] D. Polarski and A. A. Starobinsky, *Class. Quant. Grav.* **13**, 377 (1996), arXiv:gr-qc/9504030 [gr-qc].
- [68] S. Yu. Khlebnikov and I. I. Tkachev, *Phys. Rev. Lett.* **77**, 219 (1996), arXiv:hep-ph/9603378 [hep-ph].
- [69] G. N. Felder and I. Tkachev, *Comput. Phys. Commun.* **178**, 929 (2008), arXiv:hep-ph/0011159 [hep-ph].
- [70] A. V. Frolov, *JCAP* **0811**, 009 (2008), arXiv:0809.4904 [hep-ph].
- [71] D. I. Podolsky, G. N. Felder, L. Kofman, and M. Peloso, *Phys. Rev.* **D73**, 023501 (2006), arXiv:hep-ph/0507096 [hep-ph].
- [72] A. D. Dolgov and D. P. Kirilova, *Sov. J. Nucl. Phys.* **51**, 172 (1990), [Yad. Fiz.51,273(1990)].
- [73] J. H. Traschen and R. H. Brandenberger, *Phys. Rev.* **D42**, 2491 (1990).
- [74] Y. Shtanov, J. H. Traschen, and R. H. Brandenberger, *Phys. Rev.* **D51**, 5438 (1995), arXiv:hep-ph/9407247 [hep-ph].
- [75] A. D. Linde, *Phys. Lett.* **B259**, 38 (1991).
- [76] R. Kallosh, A. Linde, and D. Roest, *JHEP* **11**, 198 (2013), arXiv:1311.0472 [hep-th].
- [77] L. Delle Rose, C. Marzo, and A. Urbano, *JHEP* **05**, 050 (2016), arXiv:1507.06912 [hep-ph].